UNIVERSITY OF CALIFORNIA SAN DIEGO

Effects of B-Cell Lymphoma-6 in Skeletal Muscle Development and Metabolism

A thesis submitted in partial satisfaction of the requirements
for the degree of Master of Science

in

Biology

by

Brian Manalansan Gutierrez

Committee in charge:

Professor Ronald Evans, Chair
Professor Randolph Hampton, Co-Chair
Professor James Wilhelm

2020

The Thesis of Brian Manalansan Gutierrez is approved, and it is acceptable in quality and form for publication on microfilm and electronically:

_____

_____

Co-Chair

_____

Chair

University of California San Diego

2020

DEDICATIONS

I would like to dedicate this thesis to my family and friends for their love and support. I want to thank my mother, Emelita Manalansan Gutierrez, for constantly supporting me in my endeavors. To the Manalansan-Bunsoy family here in the U.S., the Philippines, and abroad, thank you for believing in me and for making it feel like home no matter where I am. To Apu Epe, Auntie Nor, Uncle Ben, and Uncle Boy, this is also for you and may you rest in peace. To Auntie Adel, this work is to help find treatments for your illness. To all my friends that supported me throughout college, thank you for offering me help and guidance. Thank you to my KP family, Vanessa Cancio, Chau Le, Kimberly Apolonio, Josephine Reyes, Kysha Mercader, especially Leony Mijares, Carl Hermès Castillo, Gilmer Navarro, Patrick Cosare, Virgil Wong, Vinci Reyes, Nathan Au-Yeung, Nikka Faustino, and Aaron Gabriel for being a big part of my journey. I appreciate all of my friend groups from high school that have retained me and who have stayed with me up to this point. Thank you to God and to my INC family for giving me the faith to persevere and never leaving my side.

TABLE OF CONTENTS

Signature Page.....iii

Dedication.....iv

Table of Contents.....v

List of Figures.....vi

List of Abbreviations.....vii

Acknowledgments.....xi

Abstract of the Thesis.....xii

Chapter I – BCL6 and Skeletal Muscle Development.....1
Chapter I – Results.....9

Chapter II - BCL6 and PPARδ in Skeletal Muscle Metabolism.....16
Chapter II - Results.....25

Methods…….....28

Discussion.....35

References.....38

LIST OF FIGURES

Figure 1: Crystal Violet Assay stain and quantification displaying decreased number of myoblasts in FX1-treated group.....9

Figure 2: Jenner-Giemsa stain and quantification of C2C12 differentiated myotubes displays a decrease in differentiated myotubes among the FX1-treated group.....10

Figure 3: qPCR analysis of key apoptotic and cell cycle genes in proliferating C2C12 myoblasts 12

Figure 4: Western Blots with BCL6 inhibition displaying protein expression from key genes related to skeletal muscle differentiation in differentiating C2C12 myotubes.....13

Figure 5: Agilent Seahorse XF Cell Mito Stress OCR:ECAR ratio for 7 day differentiated C2C12 myotubes after 24 hour treatment exposure.....25

Figure 6: Agilent Seahorse XF Cell Mito Stress OCR:ECAR ratio for 7 day differentiated wildtype primary myotubes after progressive 7 day treatment exposure with PPARδ Agonist (MA204) 26

ABBREVIATIONS

BCL6 = B-Cell Lymphoma-6

BTB = Broad-Complex, Tramtrack, Bric a brac

HDAC = histone deacetylases

qPCR = quantitative polymerase chain reaction

OCR = oxygen consumption rate

ECAR = extracellular acidification rate

SMRT = silencing mediator of retinoic acid and thyroid hormone receptor

NCoR = nuclear receptor corepressor

PEST = proline, glutamic acid, serine, threonine

kD = kilodalton

H3K27 = histone 3 lysine 27

DNA = deoxyribonucleic acid

RNA = ribonucleic acid

B-NHL – non-Hodgkin's lymphoma of B-cell type

K_D = equilibrium dissociation constant

PPARα = peroxisome proliferator-activated receptor alpha

PPARδ = peroxisome proliferator-activated receptor delta

Cdk = cyclin-dependent kinase

Rb = retinoblastoma

BAX = Bcl2 associated X

MyoG = myogenin

Myf6 = myogenic factor 6

PGC1α = peroxisome proliferator-activated receptor gamma coactivator 1-alpha

MHC = myosin heavy chain

MyHC2 = myosin heavy chain 2

E-box = enhancer box

MRF = myogenic regulatory factor

MyoD1 = myoblast determination protein 1

DLB(C)Ls = diffuse large B cell lymphoma

TLR = toll-like receptors

NF-κB = nuclear factor kappa-light-chain-enhancer of activated B cells

RHD = Rel homology domain

IL-6 = interleukin-6

STAT = signal transducers and activators of transcription

IL-4 = interleukin-4

IL-1β = interleukin-1 beta

HEK293 = human embryonic kidney 293

DMSO = dimethylsulfoxide

LITAF = lipopolysaccharide-induced TNF-alpha factor

RXR = retinoid X receptor

FAO = fatty acid oxidation

FFA = free fatty acid

HDL = high-density lipoprotein

ROS = reactive oxygen species

ERK = extracellular signal-regulated kinase

TNFα = tumor necrosis factor alpha

ATP = adenosine triphosphate

MCP1 = monocyte chemoattractant protein 1

COX-2 = cyclooxygenase-2

IFNγ = interferon gamma

CVD = cardiovascular disease

KO = knockout

CD8 = cluster of differentiation 8

OXPHOS = oxidative phosphorylation

NADH = nicotinamide adenine dinucleotide

$FADH_2$ = flavin adenine dinucleotide

CoQ = Coenzyme Q

FCCP = carbonyl cyanide-4-(trifluoromethoxy)phenylhydrazone

NHL = non-Hodgkin's lymphoma

DMEM = Dulbecco's Modified Eagle Medium

FBS = fetal bovine serum

AA – Antibiotic-Antimycotic

(D)PBS = (Dulbecco's) phosphate buffered saline

EDTA = ethylenediaminetetraacetic acid

RT-qPCR = real-time reverse transcription quantitative polymerase chain reaction

RIPA = radioimmunoprecipitation assay

PI = protease inhibitor

BCA = bicinchoninic acid

DTT = dithiothreitol

TGS = tris-glycine-sodium dodecyl sulfate

PVDF = polyvinylidene fluoride

DI = deionized

BSA = bovine serum albumin

TBS = tris-buffered saline

HRP = horseradish peroxidase

ECL = enhanced chemiluminescence

bFGF = basic fibroblast growth factor

ACKNOWLEDGMENTS

I want to acknowledge Dr. Ronald Evans for allowing the opportunity to be in the lab in the Salk Institute for Biological Studies. I want to thank Lita Ong, Michael Downes, Ruth Yu, Annette Atkins, and Christi Brondos for your outstanding leadership and support. To all, thank you for the guidance you have all shown me.

I would like to thank Ryan Welch and Weiwei Fan for your never-ending support and guidance. Thank you for believing in me and not giving up on me. You have seen the potential in the work that I do and have sacrificed your time to serve as my mentors. Especially to Ryan, you have given me the opportunity to be mentored by you and you have helped me develop my critical thinking skills and various lab techniques, which helped me complete my thesis.

To my committee members, Dr. Randolph Hampton and Dr. James Wilhelm, thank you for your contributions and for the development of my thesis presentation. Thank you for the knowledge and wisdom needed for the mastery of my work.

I am acknowledging Jennifer Reiswig, Geisel Library, Jorge from the Writing Hub, Dr. Elizabeth Blomstedt, and Dr. Ashley Juavinett for helping me with my thesis in its entirety. Without your guidance and support, I could not have formulated my thesis to its full potential.

Figures 1 and 2 are reprints of material presented in Master's brevia in the Saltman Quarterly Spring 2020 Journal. A special thanks to the Saltman Quarterly editors and Dr. Ella Tour for revising my brevia and accepting my submission for publication.

ABSTRACT OF THE THESIS

Effects of B-Cell Lymphoma-6 in Skeletal Muscle Development and Metabolism

by

Brian Manalansan Gutierrez

Master of Science in Biology

University of California San Diego, 2020

Professor Ronald Evans, Chair

Professor Randolph Hampton, Co-Chair

BCL6 is an oncogene that is known as the principle driver of non-Hodgkin's Lymphoma. This gene also plays a role in skeletal muscle development, metabolism, and function. Several histologic stains, such as the Crystal Violet Assay, and Jenner-Giemsa stain identifies BCL6 pharmacology as a potent modulator of *in vitro* muscle development. There is additional evidence, based on apoptotic, cell cycle markers, and expression of differentiation genes that support this idea. To test this, a competitive inhibitor, FX1, was used to block the SMRT/NCOR corepressor complex from binding the BTB domain of the BCL6 gene. This drug was applied to C2C12 myoblasts to block this corepressor complex, which recruits HDACs to repress genes downstream the BCL6 gene. In the various stains and qPCR analysis, the drug-treated groups displayed a

decreased number of cells due to either apoptosis or a lack of cell cycle gene expression. The data and existing literature suggest that BCL6 may play a role in apoptotic pathways related to skeletal muscle development. Additionally, there are studies that link BCL6 to fatty acid metabolism and this was investigated using the Agilent Seahorse XF Mito Stress Test to measure the OCR:ECAR ratios of C2C12 myoblasts and wildtype primary myoblasts. The assay suggests that the inhibition of BCL6 results in cells utilizing glycolysis as their main fuel source, instead of fatty acid metabolism under mitochondrial stress. Further understanding of the role of BCL6 in skeletal muscle development and metabolism provides possible therapies and treatments for muscular dystrophies and metabolic diseases.

Chapter 1 – BCL6 and Skeletal Muscle Development

BCL6 Structure and Mechanism of Action

BCL6 is a transcription factor that represses gene expression through the recruitment of the SMRT and NCoR corepressor complex to its BTB domain at the N-terminus region, which serves as a motif for transcriptional regulation (Ci et al., 2008). BCL6 includes a six Krüppel-type C-terminal zinc finger motif to bind DNA and is regulated by a PEST motif when BCL6 is degraded upon phosphorylation (Nance et al., 2015). The gene encodes a 92-98 kD BCL6 nuclear phosphoprotein that is important in targeting genes related to cytokines, cell cycle regulators, and proteins related to apoptosis (Arima et al., 2008).

There are 2 mechanisms that BCL6 utilizes to repress target genes. One of them is binding to the SMRT/NCoR complex and the second mechanism is to switch active enhancers into a set configuration through SMRT-HDAC3-dependent H3K27 deacetylation (Hatzi et al., 2013). HDAC3 removes the acetyl from H3K27 in order to condense DNA and block the recruitment of RNA polymerase II. This allows enhancers to be switched "on" and "off" by having the BCL6-SMRT complex compete with histone acetyltransferase, p300.

BCL6 human proto-oncogene was first looked at in studies of chromosomal breakpoints involving the 3q27 in diffuse large B-cell lymphomas (Arima et al., 2008). This rearrangement of genes is apparent in non-Hodgkin's lymphoma of B-cell type (B-NHL) resulting in B-cells rapidly proliferating in response to an antigen (Ohno, 2006). Knowing that BCL6 remodels the chromatin in B-cell germinal centers, this mechanism is shown to also occur in the skeletal muscle (Puvion-Dutilleul et al., 2003). This phenomenon was what led to the conclusion that BCL6 plays a role in skeletal muscle development. The histone H4 gene directs the transcription of BCL6, so if BCL6 protein expression is deregulated, the cell cycle will be disrupted (Ohno, 2006). The chromosomal

translocation in non-Hodgkin's lymphoma results in BCL6 fusing with the histone H4 gene, which increases BCL6 gene expression (Kurata et al., 2002). Increased BCL6 gene expression results in an increased level of several transcription factors crucial for lymphocyte proliferation (Kurata et al., 2002). The proliferation and differentiation of myoblasts will be analyzed to see if the inhibition of BCL6 affects the cell cycle, since it has been found that BCL6 plays a role in embryological development (Wagner et al., 2011). We will investigate the role of BCL6 in skeletal muscle development by the use of a BCL6 specific inhibitor, FX1, during myoblast proliferation or fusion (M. Cardenas et al., 2016), along with various stains to examine this effect. The C2C12 mus musculus immortalized myogenic cell line will be utilized as an *in vitro* model. However, C2C12 cells contain high variability due to their origin and the culture conditions. There is higher expression of adhesion proteins mRNAs in satellite cell-derived myoblasts than C2C12 cells indicating that there are structural and developmental differences between the two cell lines, which is why primary myoblasts were also studied to serve as a model for myogenesis *in vitro* (Hindi et al., 2017).

FX1 binds to BCL6 as a competitive inhibitor to the SMRT/NCOR corepressor complex. FX1 has a higher binding affinity to the BTB domain than the SMRT/NCOR corepressor complex with a K_D of 7 ± 3 μM compared to SMRT/NCOR with a K_D of 30 ± 3 μM (M. Cardenas et al., 2016). This was found by conducting a microthermal stability assay, which displays the amount of fluorescence that is released from a bound molecule. FX1 at a concentration of 10μM of allows for the inhibition of 80% of BCL6 activity with additional data supporting the use of 20-25 μM of the compound for maximum inhibition of BCL6 without adverse toxicity (M. G. Cardenas et al., 2016). FX1 allows us to study the effect of BCL6 in the skeletal muscle to explore therapies and treatments for various diseases. This is a quick and effective method to examine if there are any

effects in skeletal muscle development and metabolism *in vitro* with the ability to probe BCL6's role *in vivo*. This allows for the ability to test the efficacy, absorption, and safety by mimicking the subject's environment in ideal conditions. Having non-invasive experiments allows for the creation of effective delivery methods and avoid any potential toxic effects that will be administered to the subject.

Knowing that this gene is also known to play a role in adipocyte reduction and hepatic lipid metabolism (LaPensee et al., 2014), we will investigate whether skeletal muscle metabolism is also altered. BCL6 has been known to suppress fasting transcription when the repressor converges genome wide with PPARα. When BCL6 is deleted, lipid catabolism is enhanced indicating that BCL6 negatively regulates oxidative metabolism (Sommars et al., 2019). Various transcription factors have been studied with regards to their relation to BCL6, but we will be looking at the nuclear receptor, PPARδ due to its role in mitochondrial respiration. This is important when considering exercise and lipid catabolism. Another nuclear receptor, PPARα, contains a vast amount of shared regulatory regions that BCL6 binds to in response to fasting and the accumulation of lipids, resulting from the KO of this nuclear receptor, but it has been noted that PPARδ has been recruited in order to reverse the effects of lipid accumulation (Sommars et al., 2019). PPARδ will be mainly focused in the context of skeletal muscle metabolism. With the data accumulated in this project, it shows that BCL6 is a regulator of skeletal muscle development and by altering PPARδ expression, BCL6 plays a role in skeletal muscle metabolism.

The Impact of BCL6 on Proliferation

BCL6 has been identified to cause cell proliferation by repressing the Cdk inhibitors, p21 or p27, to block cell cycle arrest (Muñoz-Alonso et al., 2005). Cdks are serine/threonine kinases

that depend on the cyclin protein family to initiate the cell cycle (Malumbres, 2014). p21 and p27 also inhibit the phosphorylation of the tumor suppressor, Rb, to regulate the activity of the transcription factor, E2F. For E2F activation to occur, Rb is phosphorylated and is released from E2F, resulting in E2F driven transcription of cell cycle genes to advance the transition from G_1 to S phase (Nevins, 2001).

A reduction in cellular proliferation is controlled by two biological functions: regulating apoptosis and/or inhibition of cell cycle regulatory genes. Some of these apoptotic genes, include BAX and p21. To test whether there is a reduction in cell number due to apoptosis, gene expression should be measured about 24-48 hours prior to maximum confluency (Murphy et al., 2002). An addition technique that complements gene analysis by qPCR is the use of crystal violet staining to detect the number of cells in the visual field.

BCL6 has a role in apoptosis among lymphocytes and within myogenic cells where this proto-oncogene inhibits apoptotic cell death (Kumagai et al., 1999). As a transcriptional repressor, BCL6 represses the proliferation of lymphocytes by apoptosis within the germinal center (LaPensee et al., 2014). In addition to apoptosis, numerous signaling pathways for the cell cycle have positive-feedback loops to compensate for the decrease in cells that progress through the cell cycle (Pomerening, 2008). These signaling pathways suggests a possible feedback mechanism employed by BCL6.

The Impact of BCL6 on Differentiation

Myoblast differentiation occurs after cell cycle arrest with cell fusion to form multinucleated myotubes. This occurs when myoblasts are placed in low serum conditions, which by the loss of excess growth factors signal cellular differentiation (Tower, 2008). Among these

muscle-specific genes include MyoG and Myf6, which are involved in muscle tissue formation in embryonic development, also known as myogenesis. High gene expression from these genes indicate that myoblasts are in cell quiescence, especially among cells that are in close contact with one another (Tanaka et al., 2011).

When Cdk inhibitors like p21 are active, myoblasts undergo quiescence and commence differentiation. BCL6 undergoes a cascade through the caspase 3 pathway, which destroys cellular structures resulting in apoptosis (Kumagai et al., 1999). If this apoptotic mechanism can be altered without disrupting myogenesis, this allows for possible treatments and therapies for muscular dystrophies (Dee et al., 2002). To see if BCL6 can be altered to mitigate the effects of muscle dystrophies, we can observe muscle structural and motor proteins, myosin. Fast-twitch muscle fibers are highly glycolytic and are quick to fatigue, while slow-twitch muscle fibers are highly aerobic and are slow to fatigue. The type of muscle fiber will indicate what type of fuel is utilized and this switch is caused by exercise-induced PGC1α expression (Roberts et al., 2017). If BCL6 has a role with myosin gene expression or PGC1α expression, BCL6 can be an important regulator of skeletal muscle development and metabolism.

Skeletal muscles are classified into fast or slow-twitch muscle, based on the amount of fast-type or slow-type MHCs. The determination of fast or slow muscle fibers is based on the promoter activity of the slow MyHC2 and deletion analysis identified an 86bp segment that results in a significant decrease of slow MyHC2 promoter activity (Weimer & DiMario, 2017). The non-canonical E-box, acting as a binding site for E-protein, E47, controls the specific expression of the slow MyHC2 gene and it has been studied that MRFs, such as MyoD1 and myogenin, bind to E boxes, indicating that BCL6 potentially has a role in regulating skeletal muscle fiber types

(Weimer & DiMario, 2017). MyoD1 is one of the MRFs essential for myogenic determination, which can be manipulated to enhance or diminish MyHC expression (Sharma et al., 2018).

The Role of BCL6 in Inflammation

BCL6 is an important transcriptional repressor in the development of the germinal centers of B cells and DLBLs. Without BCL6, there is an inability to produce high affinity antibodies due to the lack of developed germinal centers. Loss of global BCL6 expression results in a severe inflammatory reaction, which is fatal in mice (M. Christopher, 2016). While BCL6 plays an important role in the differentiation of B-cells in their germinal centers, little is known about the function of BCL6 in the skeletal muscle.

In macrophages, the inflammatory response is activated by TLRs triggering signaling cascades in the NF-κB gene network. BCL6 controls this process by repressing inflammatory genes through histone deacetylation that are bound by NF-κB and the histone acetyltransferase, p300, after TLR4 is stimulated (Zhang et al., 2019). p65 is a protein that is a part of the NF-κB transcription factor family, which contains a 300 amino acid long amino-terminal RHD (Ser 276 and Ser311), where phosphorylation of Ser 276 breaks an intermolecular interaction enabling the interaction of the transcriptional coactivator, p300 (Oeckinghaus & Ghosh, 2009). This post-translational modification supports the relation between BCL6 and the NF-κB gene network. It also has been discovered that FX1 reduces the NF-κB signaling pathways allowing BCL6 to bind to target genes downstream with a higher affinity (Zhang et al., 2019). NF-κB is a central mediator of immune and inflammatory responses and in stress responses and cellular development, especially in the regulation of apoptosis and cell proliferation (Oeckinghaus & Ghosh, 2009).

Knowing that the inhibition of BCL6 leads to an enhanced affinity to target genes downstream, acute experiments can be conducted to examine its effects on the skeletal muscle.

The inhibition of BCL6 results in altered immune status due to an excessive amount of interleukins produced, which regulate the inflammatory response (LaPensee et al., 2014). Exercise causes an inflammatory response due to the skeletal muscles producing cytokines like IL-6 (Khazaei, 2012). The BCL6 DNA recognition motif is bound by STAT transcription factors mediating cytokine signaling where BCL6 could repress IL4-induced transcription (Dent et al., 1997). If STAT-responsive genes are dysregulated, inflammatory diseases can be mitigated, especially with BCL6 overexpression preventing the upregulation of IL-1β, which is known to be activated by NF-κB (D. Chen et al., 2019). Depending on the type, intensity, and duration of exercise, exercise also leads to an increase in oxidative stress but inflammation is reduced shortly thereafter (Khazaei, 2012). During exercise, the skeletal muscle releases myokines that play a function in the immune system and in adipose tissue metabolism (Ertek & Cicero, 2012). The link between the role of BCL6 in inflammation and the production of inflammatory markers during exercise helps link the importance of BCL6 in the exercising skeletal muscle.

Generating BCL6 KO Models

The utilization of molecular inhibitors will only deliver a model suitable for rendering the target protein non-functional, but it may still bind to certain molecules or form complexes. The use of a Cre-LoxP system will generate a site-specific deletion of DNA sequences between two loxP sites (Kim et al., 2018). Deleting BCL6 will show what pathways are affected within skeletal muscle development and metabolism in order to evaluate what possible therapies have not yet been discovered with this gene. However, this is a generally long process due to the amount of times

needed to breed in order to generate the appropriate recombination of the Cre-driver strain with a floxed mouse strain. The Cre-driver strain needs to express a promoter that is specific to the cell of interest prior to breeding with a floxed mouse strain (Kim et al., 2018).

Another method of generating a BCL6 KO model is to utilize adenoviral vectors to deliver a viral genome *in vitro*. This is easy to produce, and this method generates high levels of transgene expression. It is crucial to determine the adenovirus titer in order to avoid any adverse effects that may occur with excessive adenovirus. HEK293 cells are ideal to use due to their high titer platform and speed to generate proteins (Arena et al., 2019). qPCR would be conducted to quantify the amount of infection units per mL and is a quick and effective way to determine the infectious titer of new virus stocks (Thomas et al., 2006).

Chapter 1 - Results

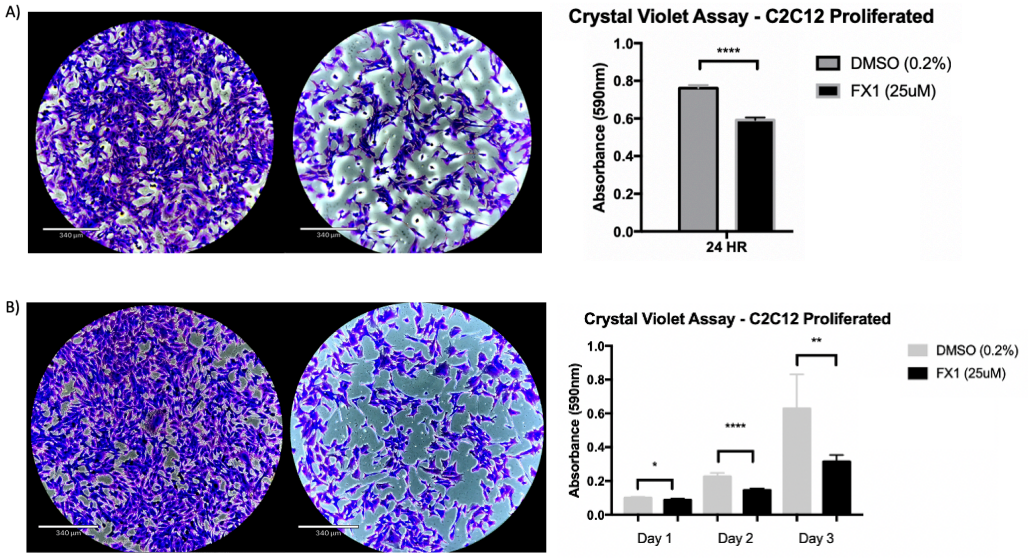

Figure 1: Crystal Violet Assay stain and quantification displaying decreased number of myoblasts in FX1- treated group. ECHO Revolve Microscope was used to evaluate the extent of proliferation of C2C12 myoblasts. The Crystal Violet Assay was conducted on C2C12 myoblasts showing the DMSO-treated group (left) and the FX1-treated group (right). Each 6-well plate sample had a seeding density of 300,000 and has been proliferating for 24 hours in either DMSO or FX1. The FX1-treated group displays a profound decrease of cells, based on the amount of stain in the visual field. n = 3, $p < 0.0001$ (****) determined by 2-tailed student t-test. The second analysis (B) had FX1 added after the first day of seeding and was stained after Days 1, 2, and 3. n=3, $p < 0.1$ (*), $p < 0.01$ (**), $p < 0.0001$ (****) determine by 2-tailed student t-test. All calculations for statistical significance in this project were done with two-tailed student t-tests between each group as determined by GraphPad Prism (Version 7).

The Crystal Violet Assay is used to test the cytotoxicity and viability of adherent cell cultures by utilizing a Crystal Violet dye that binds to proteins and RNA (Feoktistova et al., 2016). This dye is solubilized after detached cells are eliminated from the wells to measure the absorbance at 595nm. Based on the amount of dye that is present in the well, this will correlate to the number of cells that are present. The images show that BCL6 antagonism produces a profound impact on myoblast differentiation *in vitro*, but it is still unclear if this is solely due to apoptosis or due to direct inhibition of key cell cycle genes.

The Crystal Violet Assay revealed a drastic decrease in the proliferation rate with BCL6 inhibition by FX1 when compared to the control group (Figure 1A). Figure 1A shows an absorbance reading of 0.75 ± 0.016 for the control group and 0.6 ± 0.014 for the FX1 group ($p < 0.0001$). Figure 1B also shows the same phenomenon where there is a significant decrease in the proliferation rate when treated with FX1 progressively for 3 days. After 1 day of drug treatment, the DMSO were recorded as 0.100 ± 0.006 and FX1 as 0.089 ± 0.007, 2 days of drug treatment resulted in DMSO being 0.226 ± 0.022 and FX1 being 0.146 ± 0.011. With progressive treatment up to 3 days, there is still a significant decrease where DMSO had an absorbance reading of 0.629 ± 0.202 and FX1 with 0.316 ± 0.038.

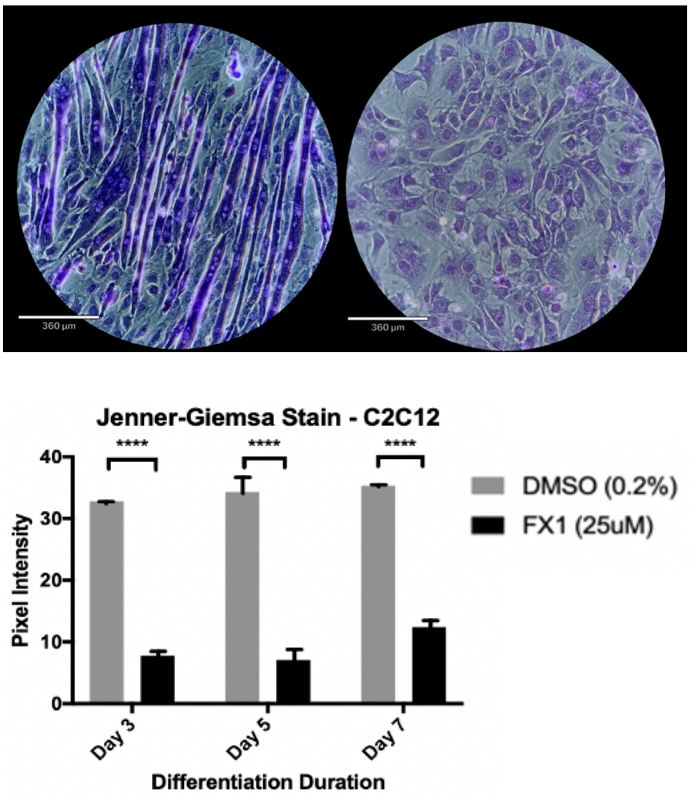

Figure 2: Jenner-Giemsa stain and quantification of C2C12 differentiated myotubes displays a decrease in myotube fusion among the FX1-treated group

The image shows C2C12 myotubes that were differentiated for 7 days. Jenner-Giemsa stain displays the multinucleated myotubes. Drug-treated group (right) lacks the amount of myotubes formed compared to the vehicle group (left). Pixel intensity was measured using ImageJ software. $n = 3$, $p < 0.0001$ determined by 2-tailed student t-test.

The Jenner-Giemsa stain indicated that FX1 completely blocked myoblast fusion. The pixel intensities reflect the amount of stain in the visual field and were measured between the DMSO vs. FX1 groups. The first day was not measured since each group was switched to differentiation media for the first day, so the results would have been negligible. On Day 3, there is a relative intensity of 32.79 ± 0.44 vs. 7.79 ± 0.29, Day 5 with 34.32 ± 0.07 vs. 7.10 ± 0.02, and Day 7 with 35.31 ± 0.02 and 12.43 ± 0.21. This data indicates that BCL6 is a crucial regulator of myoblast proliferation and differentiation *in vitro*.

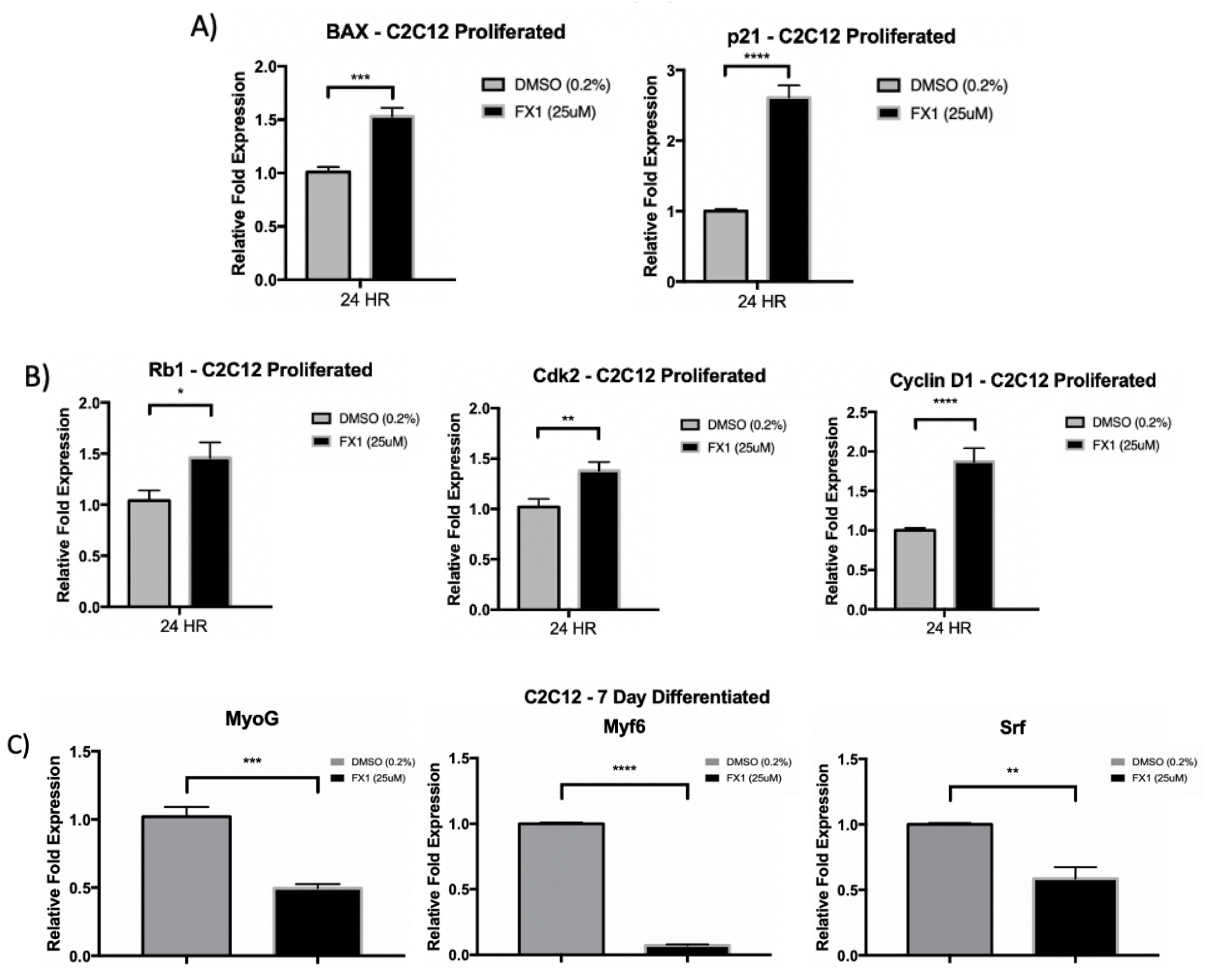

Figure 3: qPCR analysis of key apoptotic and cell cycle genes in proliferating C2C12 myoblasts. (A) Analysis of apoptotic genes with 24-hour treatment. **(B)** Analysis of cell cycle genes with 24-hour treatment. **(C)** Analysis of differentiation genes with 7-day treatment.

All genes were measured and quantified using RT-qPCR to measure the extent of C2C12 myoblast proliferation. BAX and p21 gene expression were measured to determine if the inhibition of BCL6 causing the decreased number of myoblasts was due to apoptosis. Cells were treated with either DMSO or FX1 for 24 hours. Relative fold expression was measured using the vehicle group. There was a significant increase in gene expression within the FX1 group, which indicates that apoptosis may play a role in the BCL6 pathway. BAX gene expression has about a 50% increase in gene expression with the FX1 group (DMSO, 1.01 ± 0.05; FX1, 1.53 ± 0.08; $n = 12$, $p < 0.001$ (***)). p21 had a relative fold expression of 1.00 ± 0.03 (DMSO) and 2.61 ± 0.17 (FX1); $n = 12$,

$p < 0.0001$ (****). BAX and p21 expression decreases, indicating that these proteins are regulatory and are crucial to prevent cancerous effects in various tissues.

Rb1, Cdk2, and Cyclin D1 are key cell cycle genes that were evaluated to determine whether BCL6 has a link within the cell cycle. With Rb1, there was a significant difference between both treatments (DMSO, 1.04 ± 0.10; FX1, 1.46 ± 0.15; $n = 12$, $p < 0.1$). Cdk2 is reported to have fold expression differences of 1.02 ± 0.08 (DMSO) vs. 1.38 ± 0.09 (FX1); $n = 12$, $p < 0.01$. There is a significant difference with the Cyclin D1 gene with relative fold differences of 1.00 ± 0.03 (DMSO) vs. 1.87 ± 0.17 (FX1); $n = 12$, $p < 0.0001$.

C2C12 myotubes were differentiated for 7 days, prior to RNA extraction. RT-qPCR was conducted to measure MyoG, Myf6, and Srf, which are genes crucial to myotube formation and it also indicates the cells' exit from the cell cycle. MyoG was reported to have relative fold expressions of 1.00 ± 0.01 (DMSO) and 0.24 ± 0.02 (FX1); $n = 12$, $p < 0.001$. Myf6 also shows a significant reduction with results showing 1.00 ± 0.01 (DMSO) and 0.07 ± 0.01 (FX1); $n = 12$, $p < 0.0001$. Srf data shows a significant decrease between both groups with 1.00 ± 0.01 (DMSO) vs. 0.59 ± 0.09 (FX1); $n = 12$, $p < 0.01$. The data also suggests that BCL6 is a key mediator of differentiation in the skeletal muscle.

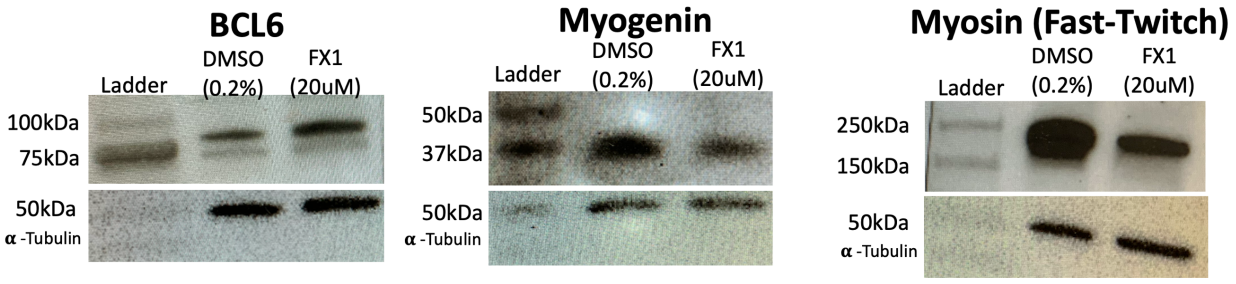

Figure 4: BCL6 inhibition regulates protein expression of skeletal muscle differentiation factors in C2C12 myotubes

2.2 x 10^6 myoblasts were seeded on 10cm^2 plates and were grown until 100% confluency prior to differentiation. Myoblasts were induced to differentiate in the presence of DMSO and FX1 for 7 days to test the impact of BCL6 on these key differentiation genes. α-tubulin, a cytoskeleton protein, was used as a loading control in order to normalize the amount of protein expression shown in each lane. Using ImageJ to quantify the relative intensities of protein expression, BCL6 has a 2.37 relative increase between the FX1-treated and DMSO groups, 1.93 relative decrease in protein expression in myogenin, and 1.73 decrease in protein expression in myosin (fast-twitch).

With the addition of FX1, it was found that the protein expression of BCL6 was increased, indicating that there is a positive feedback. BCL6 is known to interact with a transcription factor, LITAF, which is known to promote cell apoptosis and differentiation in B cell non-Hodgkin's lymphoma, where knock-down of LITAF results in the upregulation of BCL6 indicating a feedback mechanism (Shi et al., 2016). p53, a tumor suppressor protein, is known to induce the expression of BCL6, which results in the inhibition of p53 strengthening the role of BCL6 in cell proliferation (Green, 2006). BCL6 is able to bind to its own promoter to repress itself, but its negative autoregulatory circuit can be blocked by a subset of mutations located within the first noncoding exon, which affects 2 adjacent BCL6 binding sites (Pasqualucci et al., 2003). BCL6 can be manipulated to possibly control the apoptotic and differentiation mechanisms involved in the skeletal muscle.

It has been confirmed that MyoD1 regulated myoblast differentiation and forms a feedback loop with miR-501-3p, a novel muscle-specific miRNA that regulates myogenic differentiation, indicating that BCL6 may play a role in this feedback mechanism (Hou et al., 2019). This supports the idea of BCL6 playing a role in muscle regeneration, since MyoD1 is found in regenerated

muscle fibers, however, Myogenin protein expression shows a decrease in expression when BCL6 was inhibited, indicating that BCL6 is involved in a specific part of the MyoD1 pathway for differentiation. MyoD1 and myogenin are involved in the terminal differentiation of muscle fibers and have increased RNA expression after muscle injury, so these are good indicators of whether BCL6 is actively involved in any of these pathways (Füchtbauer & Westphal, 1992).

The results display that BCL6 has a significant impact in the proliferation of the skeletal muscle, as evidenced by the Crystal Violet Assay supporting the idea that BCL6 plays a role in the cell cycle. This gene also impacts differentiation, as shown with the Jenner-Giemsa stain where there is a decrease of myotube fusion indicating that BCL6 may be considered as a possible link to muscular dystrophies. The qPCR results support the conclusion that myoblast proliferation and differentiation are negatively impacted, and the Western Blot results indicate that BCL6 has an auto inducing negative feedback network to regulate its own expression. The blot also indicates that there is a decrease in myosin expression, especially with fast twitch suggesting that inhibition of BCL6 impairs skeletal muscle metabolism, since differing muscle fibers utilize different fuel sources.

Chapter 2 – BCL6 and PPARδ in Skeletal Muscle Metabolism

Introduction

Exercise has many beneficial effects, such as a prolonged quality of life, decreased risk of metabolic diseases, and enhanced performance in physical activity. Due to pervasive sedentary behavior, many people have insufficient exercise, increasing risk of Type II Diabetes, depression, and heart disease. A key nuclear hormone receptor that is essential to confer these benefits is PPARδ. There are many roles of this receptor where it has a role in lipid metabolism, inflammation, and glucose regulation (Barish et al., 2008). Different fuel sources used, such as fats or carbohydrates, will influence performance in different ways. With increased use of fats for energy, this gives increased endurance, but with reduced speed, while carbohydrates give the greater speed and power, but less endurance.

Inflammatory responses are linked to cardiovascular disease, atherosclerosis, and hepatic failure (Samavati et al., 2008). Inflammation reduces mitochondrial aerobic respiration, while enhancing anaerobic citric acid cycle, such as glycolysis and the phosphagen system. Inflammation occurs when cytokines attract immune cells, such as macrophages, leukocytes, dendritic cells, and mast cells, to reach a site of injury or foreign substance. There are anti-inflammatory properties of PPARδ when it binds to BCL6 where it represses inflammatory signaling. When PPARδ is bound to a synthetic ligand, such as fatty acids, eicosanoids, or oxysterols, the nuclear receptor and BCL6 complex is disrupted, which allows for this repression of inflammatory signaling (Smith et al. 2016). BCL6 recruits HDACs, which decreases the accessibility of the DNA bound by other transcription factors. The histones wrap the DNA more tightly, which prevents the transcription of inflammatory signaling genes.

Many metabolic diseases originate from chronic inflammation, such as atherosclerosis and cardiac hypertrophy. Atherosclerosis due to plaque buildup, there is less blood that is able to traverse throughout the body, which causes the heart to work harder due to the low stroke volume. As the heart rate increases in order to compensate for the lack of blood flow, this puts more stress on your heart, which ultimately leads to cardiomyopathy (Yu et al., 2008).

During aerobic exercise PPARδ plays a key role in muscle metabolism causing a shift to Type I muscle fibers, which have high endurance properties and increased mitochondrial density. Aerobic exercise favors use of fatty acids which supports sustained exercise relative to carbohydrates. This oxidative shift results in enhanced running performance and endurance in physical activity compared to subjects that lack this receptor. These properties of PPARδ enhance exercise performance and the mechanisms of action and functions of this receptor will be clarified at a genetic level.

Structure and Function of PPARδ

The structure of PPARδ contains specific sequences that are important in the regulation of metabolic processes and diseases. These sequences contain conserved regions within the ligand-binding domain that is crucial for the binding of various molecules, such as agonists or antagonists. When this region is bound to a molecule, the Histone 2'-Histone 3 surface segment is reorganized which was found through the use of X-Ray crystallography (Wu et al., 2017). Researchers were able to create molecules that will bind to this region and one of these would be the PPARδ agonist, GW501516, which activates the receptor to enhance the expression of downstream target genes. Some endogenous ligands include fatty acids and eicosanoids, which are polyunsaturated fatty acids. This class of agonist initiates a conformation change where hydrogen bonds between

carboxyl groups and hydrophilic side chains are made to stabilize the ligand to the receptor (Wu et al., 2017).

PPARδ is able to heterodimerize with the RXR, which causes lipid catabolism and increases insulin sensitivity when a ligand is present (Chen and Yang, 2014). This mechanism enhances muscle performance by inducing fatty acids and glucose muscle uptake in order to increase energy metabolism. PPARδ is also able to form a complex with BCL6, which promotes inflammation, but if a ligand is bound to PPARδ, it disrupts this complex and BCL6 is able to continue repressing genes downstream and maintain its anti-inflammatory properties (Liu et al. 2018). Many processes are influenced by ligand-binding domains depending on whether it is bound by an inhibitor or activator.

The Role of PPARδ in Fatty Acid and Carbohydrate Metabolism

Knowing that PPARδ increases fatty acid catabolism, fatty acid oxidation (FAO) is increased by the surplus of circulating FFAs. With the increase of FFAs that are mobilized, physical endurance is enhanced which allows for better performance in aerobic exercises, such as running, swimming, or cross-country skiing (Barish et al. 2006). Secondary and primary signaling pathways from exercise increases mitochondrial gene expression to promote mitochondrial biogenesis to meet the metabolic demand.

PPARδ is thought to mitigate insulin resistance by utilizing excess glucose for the pentose phosphate pathway to generate fatty acids (Lee et al. 2006). This results in the creation of HDLs, which recycles cholesterol back to the liver (Monsalve et al. 2013). Recycling the cholesterol from the blood vessels decreases plaque buildup and allows for proper blood flow to tissues, thus reducing complications due to atherosclerosis and coronary heart disease.

Enhancing Muscle Endurance by PPARδ

There are three main types of skeletal muscle fiber types, which are Type I, Type IIa, and Type IIx, in humans. Type I fibers have high mitochondria density and favors aerobic respiration, resulting in more endurance due to the high capacity of fatty acids as fuel. Type IIx muscle fibers are glycolytic and are faster to fatigue due to the limited source of glucose that is available for these muscles resulting in higher exercise power, which are prevalent in sprinters and power lifters. Type IIa intermediate muscle fibers contain the qualities of both Types I and IIx. These muscle fibers are slow-twitch fibers meaning that they are slow to fatigue. These fibers are trainable and are able to switch to different types depending on the type of physical activity done, especially transitioning from a powerlifter to a long-distance runner.

PPARδ is one of the master regulators for Type I muscle fiber switching. Transgenic mouse studies have been conducted where PPARδ overexpression displayed an increase of oxidative Type I muscle fibers present in the skeletal muscle when compared to the wild type litter mates (Wang et al. 2004). It can be seen that the amount of red pigmentation within the tissue indicates increased oxidative metabolism. These are the main properties of muscle fiber types switching to Type I (Wu et al. 2017). Type I fibers are prevalent in endurance athletes, such as long-distance runners and cross-country skiers. In addition, the rate of oxygen consumption, VO_2 max, has a positive correlation with the amount of Type I fibers (Wilson et al. 2012). Increased interval training combined with higher intensity exercise causes an increase in VO_2 max indicating that VO_2 max is trainable resulting in increased muscle mitochondrial content and capillary density due to the increased need of oxygen to the muscle (Bacon et al., 2013).

The Heart and Exercise Performance

The heart is vital in exercise performance because it is what delivers oxygenated blood to various tissues, while pumping deoxygenated blood to the lungs. Cardiac output is the amount of blood that flows through the heart at a certain heart rate and given stroke volume. This stroke volume can be increased after training, which allows for greater cardiac output, thus enhanced exercise performance.

The inability to exercise, as a result of heart failure, is perhaps due to the dysfunction of oxidative metabolism in the skeletal muscle (Zizola et al. 2015). An 8-week study was conducted on C57BL/6 mice induced with a myocardial infarction, thus developing ventricular dysfunction. Two groups were randomized to receive either PPARδ agonist, GW501516, or a placebo for the 8 weeks. The results indicated that the agonist rescued oxidative and fatty acid metabolism, which restored proper exercise activity, despite having left ventricle dysfunction (Zizola et al. 2015).

It was seen in another study by Yu et al. that diabetic hearts with high lipid contents resulted in a decrease in PPARδ. Cardiomyopathy is a disease of the heart that decreases cardiac output due to the decrease of the volume of blood pumped out of the heart caused by excessive cardiac tissue. It is suggested that cardiomyopathy is caused by ROS and ERK that is activated by hyperglycemia-induced cell hypertrophy (Yu et al. 2008). These cause hyperglycemia, or the elevation of blood glucose, which results in cardiomyopathy.

Hyperglycemia causes oxidative stress due to the accumulation of ROS, which are radicals that damage macromolecules important for metabolic function. Excess glucose reacts with plasma proteins forming advanced glycation end products, which triggers the production of ROS causing increasing inflammation (Wright et al., 2006). These radicals are highly reactive with lipids, proteins, and nucleic acids. With ERK activation, this causes hypertrophy, thus increasing cell

size. When inhibiting ERK activation in hyperglycemia-treated cells, it was seen that PPARδ expression was not reduced (Yu et al. 2008). An excess amount of cardiac tissue makes it difficult for blood to pump out of the heart.

Anti-Inflammatory Properties of PPARδ

Exercising causes acute inflammation, especially from creating muscle tears after physical activity. To recover from exercise-induced stress, the inflammatory response from chemokines recruits immune cells to the damaged site to repair the muscle fibers. It is known that during acute inflammation, oxidative metabolism is affected and there is a shift in fuel usage to carbohydrates (Samavati et al. 2008). The pro-inflammatory cytokine, TNFα, is important in modulating this response. TNFα is a contributor to atherosclerosis and metabolic dysfunction because it binds to its receptor impacting the downstream signaling cascade that affects the ATP synthesis pathway in oxidative phosphorylation. Once TNFα binds to these receptors, there is an increase of ROS, which will impair oxidative phosphorylation for the generation of ATP (Samavati et al. 2008).

PPARδ alleviates this inflammatory response by inhibiting TNFα (Smith et al. 2016). Other inflammatory genes include MCP1, IL-6, and COX-2. Smith et al. showed that inducing 2 Mia PaCa-2 human pancreatic cancer cell groups with either TNFα or TNFα and PPARδ agonist, GW501516, results in a decrease in the relative mRNA expression of the given inflammatory genes, stated above. PPARδ also suppresses the inflammatory responses produced by IL-1β and IFNγ indicating that PPARδ is a regulator of the inflammatory response (Barish et al., 2008).

BCL6 is a factor in the inflammation process where it represses proinflammatory cytokine genes, but when a complex is formed with PPARδ, this repression does not occur (Liu et al. 2018). When a ligand binds, this complex is disrupted allowing for the regulation of the inflammatory

response. This will greatly enhance oxidative phosphorylation and mitochondrial function since oxygen utilization is not affected due to an increased production of ROS (Samavati et al. 2008). When exercise occurs, natural ligands, such as free fatty acids, bind to PPARδ, which reduces inflammation. In summary, exercise reaps many benefits, especially with those that have CVD, respiratory problems, or oxidative stress, since there is less stress on the subject (Ertek and Cicero 2012). Exercise helps relieve stress with the release of endorphins and endogenous endocannabinoids, as well as mitigate the inflammatory responses that is common to CVD and atherosclerosis.

BCL6 and Lipid Metabolism

One of the consequences of the oncogenic properties of BCL6 is the reduction of adipose tissue due to the increased uptake of fatty acids for B-cell proliferation (LaPensee et al., 2014). BCL6 is sequestered and bound to an unliganded PPARδ resulting in BCL6-PPAR genomic co-localization (Sommars et al., 2019). PPARα is known to be the predominant isotype in the liver, but PPARδ still physically interacts with BCL6 indicating that there is a competition between PPARα and PPARδ since they both bind to common response elements. There are 87 genomic sites where BCL6 and PPARδ are co-localized without PPARα offering the notion that this relation may be crucial for oxidative metabolism in the skeletal muscle (Sommars et al., 2019). Within BCL6 KO models, gluconeogenesis is significantly reduced and fatty acid biosynthetic genes are downregulated indicating that BCL6 is a regulator of adipocyte metabolism and insulin sensitivity (Senagolage et al., 2018).

The Relation Between BCL6 and the Electron Transport Chain

BCL6 represses genes involved in glycolysis in $CD8^+$ T cells resulting in the switch to aerobic glycolysis, as well as mitochondrial fatty acid oxidation in $CD8^+$ T memory cells (Oestreich et al., 2015). T cells rely on mitochondrial OXPHOS to generate ATP and they have a high bioenergetics demand (Salmond, 2018). When comparing skeletal muscle development with immortal cell lines, the cells share some biochemical homology concerning proliferation. Cancer cells have increased glucose uptake, despite having functional mitochondria, resulting in the Warburg effect (Liberti & Locasale, 2016). This phenomenon can be seen when BCL6 is inhibited, as evidenced in its role in skeletal muscle development. Even with functional mitochondria, skeletal muscle cells would be utilizing glycolysis as the main source of energy when BCL6 is inhibited.

Due to BCL6 being a regulator of T cell metabolism, the role of BCL6 in skeletal muscle metabolism will be investigated to determine if there is a similar mechanism that occurs. The electron transport chain will be manipulated in order to determine if BCL6 is crucial for a certain complex within the electron transport chain. NADH and $FADH_2$ are products from the citric acid cycle and supply electrons for oxidative phosphorylation. The free energy released from these electron carriers drives the synthesis of ATP (Lodish et al., 2000). The electrons flow through the four inner membrane multiprotein complexes: succinate-CoQ reductase (Complex I), NADH-CoQ reductase (Complex II), $CoQH_2$-cytochrome *c* reductase (Complex III), and cytochrome *c* oxidase (Complex IV). Complex V transfers the electrons to O_2 to form H_2O and ATP synthase catalyzes the production of ATP from ADP. The oxidation of these electron carriers can only be done if there is sufficient ADP present to generate a proton-motive force to power ATP synthesis (Lodish et al., 2000).

Oxygen consumption rate (OCR) is the measurement for mitochondrial function and the respiratory rate needed to sustain ATP production can be measured by adding the Complex V inhibitor, oligomycin (Ruas et al., 2016). By adding the protonophore, FCCP, the maximal respiration rate of the cell can be measured because the mitochondrial membrane potential will be chemically dissipated resulting in maximal OCR (Ruas et al., 2016). The collapse of the proton gradient and the spare respiratory capacity are able to be calculated, based on the basal respiration rate. Disrupting Complex I by using Rotenone and Complex III by using Antimycin A will decrease relative cell viability and will determine the proton leak, which can be a sign of mitochondrial damage and oxidative stress (Wang et al., 2015). This is the basal respiration that is not coupled to ATP production and by inhibiting Complex I and III, the independent mitochondria respiration can be determined.

Mitochondrial function has been researched in relation to NHL, which has been shown to be caused by the chromosomal rearrangement of BCL6. CD20, a signature B-cell differentiation antigen, was shown to function in B-cell growth and is part of an ion channel complex crucial for transmembrane calcium flux (Vilventhraraja et al., 2016). Anti-CD20 antibodies have been used to treat diffuse large B cell lymphoma (DLBCL), a type of NHL, resulting in an increase in the maximal respiratory capacity (Vilventhraraja et al., 2016). OXPHOS inhibitors have been utilized causing a decrease in basal oxidative phosphorylation, thus disrupting the maximal respiratory capacity of the cell line. If a dysfunctional BCL6 gene causes DLBCL, manipulation of mitochondrial respiration, as seen in NHL, BCL6 may also serve as a possible therapy for mitochondrial disease.

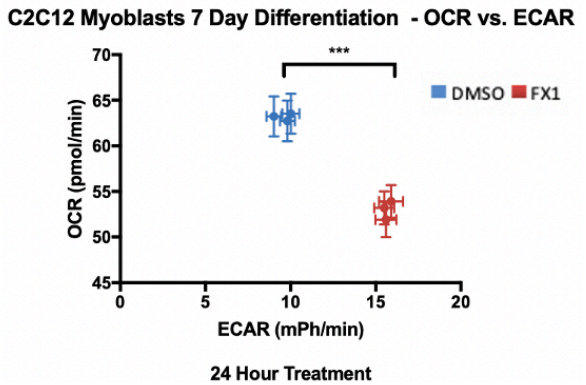

	OCR	ECAR
DMSO	63.33 ± 2.21	9.5 ± 0.46
FX1	53 ± 1.84	15.67 ± 0.63

Figure 5: Agilent Seahorse XF Cell Mito Stress OCR:ECAR ratio for 7 day differentiated C2C12 myotubes after 24 hour treatment exposure

Agilent Seahorse XF Cell Mito Stress Test was conducted on C2C12 myotubes after 24 hours of treatment. All cells were differentiated for 7 days prior to treatment. FX1-treated group shows a decrease in OCR and an increase in ECAR. $n = 36$, $p < 0.001$ (***) determined by 2-tailed student t-test. OCR and ECAR values were measured using Wave Software and statistical significance was calculated using two-tailed student t-tests between the two groups as determined by GraphPad Prism (Version 7).

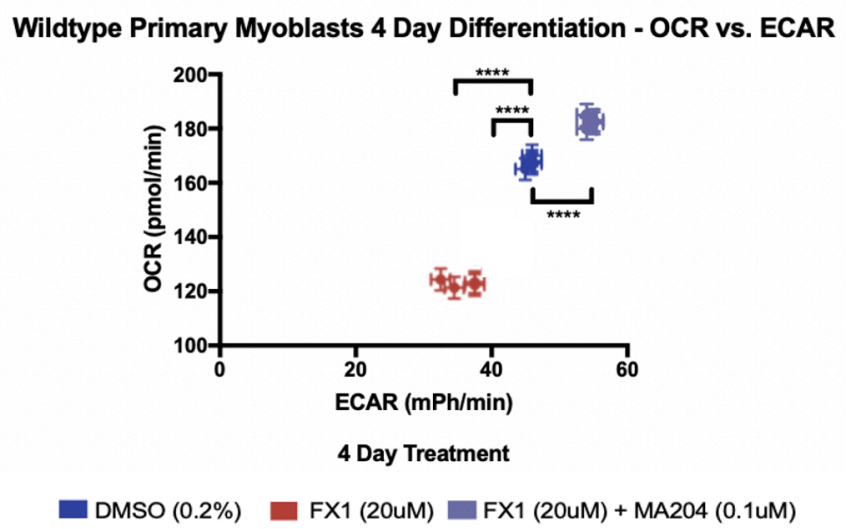

	OCR	ECAR
DMSO	167.5 ± 1.43	45.75 ± 1.43
FX1	123.5 ± 1.43	35 ± 1.43
FX1 + MA204	182.5 ± 1.43	54.5 ± 1.43

Figure 6: Agilent Seahorse XF Cell Mito Stress OCR:ECAR ratio for 4 day differentiated wildtype primary myotubes after progressive 4 day treatment exposure with PPARδ Agonist (MA204).

Wildtype primary myoblasts were differentiated for 4 days prior to conducting the assay. There were 4 treatments: DMSO, FX1, and FX1 + MA204. FX1 + MA204 shows that there is a rescue in OCR, $n = 24$, $p < 0.0001$ (****) determined by 2-tailed student t-test. Statistical significance of two-tailed student t-tests between each group as determined by GraphPad Prism (Version 7).

OCR and ECAR values were measured using Wave Software and were plotted using GraphPad Prism (Version 7). The group treated with DMSO was used as the control when assessing the effect of the OCR:ECAR ratio. The average values were calculated from 3 groups of each treatment group as indicated in the table for 4A. Figure 4B shows the values reported from 4

groups of each treatment as indicated in the table. There was a significant difference from each group compared to the DMSO group.

Methods

C2C12 Cell Culture and Differentiation Treatment

C2C12 immortalized myoblast cells are adherent and are able to grow on plastic culture dishes. These myoblasts are proliferated in myoblast growth medium containing DMEM, 10% FBS (Gibco), and 2X AA (Gibco). 10^6 cells are plated on $10cm^2$ plates with 10mL of myoblast growth medium and were placed in a CO_2 incubator at 37°C. When myoblasts are about 60% confluent, the cells were washed with 1X PBS (Corning) and were split with 1mL of 0.25% Gibco Trypsin-EDTA (1X) and placed in a CO_2 incubator at 37°C for about 5 minutes or until cells have been detached prior to transferring onto a new $10cm^2$ plate with fresh growth medium. The cells must not be fully confluent because the cells may start to fuse and partially differentiate upon cell-cell contact. For experimental assays, cells were grown for approximately 3 days or just before maximum confluency.

For differentiation treatment, myoblasts grown to maximum confluency prior to the addition of differentiation media. After washing with PBS, the myoblasts were treated with DMEM with 2% donor equine serum (Gibco) and 2% AA (Gibco) and were allowed to differentiation into myotubes up to 7 days prior to extraction.

Real-Time Reverse Transcription Quantitative Polymerase Chain Reaction

Qiagen RNA protocol was followed for RNA extraction. Media was aspirated from the wells and washed with 1mL of PBS. 350 uL of RLT buffer was added to each well to lyse the cells. Each plate was placed on a shaker at room temperature for 5 minutes. The lysate was transferred to a QIAshredder and was spun down in centrifuge at max speed for 1 minute. The lysed cells were transferred into a 1.5uL Eppendorf tube. Afterwards, 350uL of 70% ethanol was

added to each sample and was pipetted up and down to thoroughly mix. This mixture was transferred to a pink RNEasy Mini spin column for washing and after each spin down, the flow-through was discarded. The lysate was spun down for 30 seconds at 8000xg. 700uL RW1 buffer was placed into the column and spun down for 30 seconds at 8000xg. Afterwards, 500uL of RPE buffer was added to each column and spun down for 30 seconds at 8000xg, then 1 minute at 8000xg. The lysate was placed in a fresh collection tube in order to dry the column. This was done by spinning it down at max speed for 2 minutes. The column was placed in a 1.5mL Eppendorf tube and 30uL of RNAse-free water directly on the membrane. The column was incubated at room temperature before spinning down for 1 minute at maximum speed to elute the RNA. The concentration and 260nm/280nm absorbance reading were measured using a Nanodrop RNA spectrophotometer by Thermo Scientific in order to determine how much RNA to use for each sample and to test its purity.

The Bio-Rad iScript Reverse Transcription Supermix for RT-qPCR protocol was used to quickly analyze gene expression. Each sample requires 4uL of iScript RT Supermix, 1ug of RNA from each sample, and nuclease-free water, in order to work up the solution to 20uL. Each mixture was placed into a PCR machine and heated to 95°C for 5 minutes. Afterwards, each sample was lowered to 45°C allow the primers to bind during the annealing step. The final step is extension where each sample was raised to 72°C for 1 minute in order for the DNA polymerases to extend the primer sequences.

After the cDNA was obtained, the qPCR Mastermix was made to increase the number of samples for statistical analysis. Each sample requires 5uL of 2x SYBR Green (Bio-Rad), 0.5uL of the gene target's forward and reverse primers (5uM), and 1.5uL of molecular grade water. To avoid loss of volume from pipetting, 15% excess of mastermix was created. The cDNA was diluted

1:5 as the stock solution, which was then diluted to 1:10 to serve as the working solution. All samples were kept on ice in standard 1.5mL tubes. The cDNA was spun down and 3uL of cDNA was added into designated wells in a 384-well plate. 7uL of mastermix qPCR was added into each well.

Western Blot

All steps must be conducted on ice to prevent denaturation. Prepare a chilled Protease Inhibitor Cocktail (Fisher: PI78437) and create 1:100 dilutions in chilled RIPA buffer. As the centrifuge was cooling to 4°C, the 10cm^2 plate of cells was washed with cold PBS, prior to removal with a cell scraper. The cells were transferred to a chilled 1.5mL tube and 700uL of cold PBS was added to the plate prior to scraping the remaining cells into the chilled tube. The tube was spun at 500xg for 5 minutes at 4°C. The excess PBS was aspirated and 200uL of RIPA/PI was added to the tube. The mixture was pipetted 10-15 times or until solubilized to lyse the cells. The tube was spun at 140,000 RCF for 40 minutes at 4°C. Supernatant was transferred to a chilled tube and kept on ice, prior to the determination of protein concentration by the BCA Protein Assay.

Pierce BCA Protein Assay protocol was followed to prepare the standards and dilutions needed to determine protein concentration of the samples. The BCA Working Reagent was diluted to 50 parts of BCA Reagent A to 1 part BCA Reagent B. A volume of 25uL of each standard and sample was diluted 1:10 into a microplate well. 200uL of the Working Reagent was added to each well and the plate was mixed on a shaker for 30 seconds, prior to covering and incubating in 37°C for 30 minutes. After 30 minutes, the plate was cooled to room temperature. Each standard and sample was measured at 562nm and each absorbance reading was used to create a standard curve to determine the concentration of each sample.

Multiple aliquots of each sample were made to prevent repeated freeze thawing. In preparation of immunoblotting, Laemmeli buffer was prepped by adding 1M DTT at 1:20 dilution and 1:1 ratio of 2x Laemelli buffer was added to diluted protein. All samples were heated for 5 minutes at 95°C. A 10-well gel was set up in a gel trough with 1X TGS buffer and 10uL of Kaleidoscope protein ladder was used to serve as an indicator of protein size. Each sample was loaded carefully, and the gel was running at 100V, 3 Amps, and 300W just until the blue dye runs off the gel. Afterwards, the proteins were transferred by Trans-Blot Turbo PVDF using a standard 30-minute transfer. All air bubbles were rolled out to minimize interference. The membrane was washed with DI water before being blocked in 2% BSA overnight in a cold room on a rocker. This will allow the membrane to be clear of any debris. The membrane was washed with TBS three times for 10 minutes each, prior to the addition of the primary antibody of choice diluted to 1:1000 in blocking buffer for 1 hour overnight on a rocker in a cold room. After that, the membrane was washed three times with TBS for 10 minutes each before incubating the blot with an HRP tagged secondary antibody diluted 1:5000 in blocking buffer 1 hour at room temperature. Each membrane was washed three times with TBS for 10 minutes each on a rocker to eliminate any excess antibody.

The Bio-Rad Chemidoc Imaging Protocol from Image Lab software was used after incubating the blot with the antibody of choice. 1mL of ECL solution was added to the membrane. Each blot was imaged 30 times for 5 minutes using Chemidoc and the colorimetric protocols. Afterwards, each membrane was rinsed with 10mL of TBS and stored for 1 week at 4°C for additional protein analyses.

Crystal Violet Assay

C2C12 myoblasts were seeded at 35,000 per well in a 12-well plate in triplicate in DMEM, 10% FBS (Gibco), and 2X AA (Gibco). Cells were treated with a 0.2% DMSO vehicle or drug-treatment with FX1 at 25uM in media. After 72 hours, before cells were confluent, they were washed with 1X PBS (Corning). Cells were fixed in 1mL of 4% paraformaldehyde in PBS for 15 minutes. Each well was washed once with water to eliminate the fixative solution.

A stock solution of 0.1% crystal violet was created by dissolving 50 mg crystal violet powder in 10% ethanol. Afterwards, the stain was aspirated and washed 3 times with water to eliminate excess staining. After washing, the cells were left to dry. Then, 2mL of 10% acetic acid was added to each well and incubated for 20 minutes while shaking. A 1:4 dilution in water was conducted and the wells were measured at an absorbance at 590nm to determine cell density.

Jenner-Giemsa Stain

Quantifying the extent of differentiation is based on the amount of myotubes stained with Jenner-Giemsa stain. 50,000 C2C12 myoblasts were plated in 6-well plates and were differentiated with DMEM, 10% FBS (Gibco), and 2X AA (Gibco). There was one vehicle group (DMSO) and one drug-treated group (FX1). Cells were incubated in 37°C and 5% CO_2 until 100% confluency. Media was switched to DMEM with 2% horse serum (Gibco), and 2X AA (Gibco) and incubated in 37°C and 5% CO_2. C2C12 myotubes were analyzed at Day 1, 3, 5, and 7 post serum withdrawal to quantify the extent of myogenesis progressively.

Prior to quantification, cells were washed with DPBS and fixed with 100% methanol for 5 minutes. The plates were left out to air dry for 10 minutes. Jenner Stain Solution (Sigma-Aldrich) was diluted 1:3 in 1mM sodium phosphate buffer (pH 5.6). 1 mL of this dilution was placed in

each well and the cells were incubated for 5 minutes. Each well was washed with deionized water then incubated in 1mL Giemsa stain diluted to 1:20 in 1mM sodium phosphate buffer (pH 5.6) for 10 minutes in room temperature. The stain was washed with water before photographs were taken.

ECHO Revolve Microscope was used to image each well. To quantify the extent of myogenesis, ImageJ was used to identify the amount of intensity emitted from the Jenner-Giemsa stain in the myotubes. A dark purple stain will identify the multinucleated myotubes.

Agilent Seahorse XF Cell Mito Stress Assay

This assay measures mitochondrial function as it measures OCR and ECAR using electron transport chain inhibitors, oligomycin, FCCP, rotenone, and antimycin. A day prior to the assay, 20,000 wildtype myoblasts were plated in the Seahorse XF Cell Culture Microplate using Ham's F-10 Nutrient Mixture with 20% FBS, 2X AA, and 10ng/mL of basic fibroblast growth factor bFGF. Cells were treated with a 0.2% DMSO vehicle or drug treatment with FX1 at 25uM in media. A sensor cartridge was hydrated overnight in Seahorse XF Calibrant at 37°C in a non-CO_2 incubator overnight.

The assay medium was prepared the next day by using Seahorse XF DMEM medium. It was supplemented using 1mM pyruvate, 2mM glutamine, and 10mM glucose. The medium was set to pH 7.4. Prior to use, the assay medium was warmed to 37°C in a water bath. The inhibitor stock solutions and working solutions were created. Each solution was loaded into the ports on the sensor cartridge following the protocol guidelines. The microplate was prepared for the assay by replacing the growth medium to the warmed assay medium and placing it into a 37°C non-CO_2 incubator for 1 hour.

The calibration plate with the loaded sensor cartridge was placed in the instrument tray for calibration. After calibration, the calibration plate was replaced with the cell culture microplate. The Seahorse XF Mito Stress Test Report Generator will automatically calculate the Seahorse XF Cell Mito Stress Test parameters from Wave data, which has been exported to Microsoft Excel. The data was analyzed in order to determine the OCR/ECAR ratio from each sample.

Discussion

BCL6 is a transcription factor that is a crucial regulator in the development of skeletal muscle. When the SMRT/NCOR corepressor complex is blocked from BCL6, the results show that this causes an impairment of skeletal muscle development. The results indicate that BCL6 may serve as a therapeutic target to treat muscle wasting or enhance healing if utilizing either a BCL6 agonist or genetic overexpression. Knowing that BCL6 plays a role in adipocyte reduction and hepatic lipid metabolism, BCL6 activity may also affect metabolic activity in the skeletal muscle.

As evidenced by the cell cycle genes, BCL6 definitely is part of a pathway that influences the proliferation of skeletal muscle cells. The impairment of myoblast proliferation by BCL6 inhibition can be seen with the Crystal Violet Assay. It is still unclear if this impairment is due to apoptosis or the inhibition of genes important for regulating the cell cycle. The results show that both cyclin and apoptotic genes are impacted by BCL6 with the proposed mechanisms and feedback loops. BCL6 also effects the differentiation rate of myotubes, as shown in the Jenner-Giemsa stain, based on the lack of multinucleated myotubes that form. The key genes important for cell differentiation, MyoG, Myf6, and Srf, have decreased relative RNA expression.

The Agilent Seahorse XF Mito Stress Test showed that there is a shift in fuel usage from an aerobic to a glycolytic state. This was evidenced by the OCR:ECAR ratio of the drug-treated group showing a decreased OCR. In the 24-hour treatment group, the FX1 treated group had a decreased OCR, while having an increased ECAR suggesting that BCL6 mediates glycolytic and fatty acid substrate utilization. If treated progressively with a BCL6 inhibitor, OCR decreases, as well as a decreased ECAR suggesting that BCL6 definitely has a role in fatty acid oxidation. When

utilizing a PPARδ agonist, MA204, there is a rescue in the OCR indicating PPARδ is not fully dependent on BCL6 for oxidative metabolism.

The role of PPARδ has many benefits related to exercise and lifestyle. It has been discussed that this nuclear receptor is important for enhancing exercise performance, especially in endurance activities and causing a shift to Type I oxidative muscle fibers (Wu et al., 2017). PPARδ's interaction with RXR and BCL6 shows that this nuclear receptor is a regulator in biological processes, such as lipid metabolism, inflammation, and insulin sensitivity (L. Chen & Yang, 2014). Activating this nuclear receptor can serve as a therapy for atherosclerosis, heart disease, and reducing oxidative stress (Ertek & Cicero, 2012). Using agonists, such as GW501516 or MA204, serve as a therapy for treating individuals experiencing these symptoms since it will enhance the expression of anti-inflammatory genes and help regulate oxidative metabolism by reducing the amount of ROS and TNFα (Smith et al., 2016). Without PPARδ, the effects of endurance decreases, as well as the number of oxidative enzymes available for aerobic respiration to occur (Wu et al., 2017).

There is not much known to what the natural ligand is that binds to PPARδ. It is a variety of molecules, such as fatty acids or eicosanoids, that binds to PPARδ, since this nuclear receptor plays a role in many pathways for regulatory processes important for metabolism. It will be interesting to see where BCL6 plays a role with PPARδ in the skeletal muscle other than just repressing inflammatory genes because it was discussed that BCL6 recruits HDACs, which makes the DNA inaccessible due to histone binding. However, a synthetic molecule, FX1, binds to the BTB domain of BCL6 and competitively inhibits a corepressor complex from recruiting the HDACs and SMRT (M. G. Cardenas et al., 2016). This inhibition opens a discussion of what PPARδ's role is with BCL6 in the skeletal muscle.

Enhancing or silencing BCL6 gene expression and nuclear receptor, PPARδ, will help us understand their role in exercise metabolism offering an opportunity in exploring the world of exercise mimetics. BCL6 can possibly be an essential factor in skeletal muscle development and metabolism supporting the role of exercise mimetics in mimicking the benefits of exercise without actually exercising. This is useful in individuals who have muscular dystrophy or an inability to exercise due to existing medical conditions. It is proposed that the enhancement of PPARδ will help increase running time and endurance (Wu et al., 2017). With the benefits that PPARδ has on diminishing the symptoms of metabolic diseases, thus resulting in a high quality of life, there is much more to learn about the pathways that are involved to develop treatments for those that are unable to exercise. Once the full role of BCL6 is understood, possible therapies can be used to further resolve issues such as muscular dystrophy and possibly lead to exploring the shift from aerobic to anaerobic metabolism and muscle fiber type switching.

References

Arena, T. A., Chou, B., Harms, P. D., & Wong, A. W. (2019). An anti-apoptotic HEK293 cell line provides a robust and high titer platform for transient protein expression in bioreactors. *MAbs*, *11*(5), 977–986. https://doi.org/10.1080/19420862.2019.1598230

Arima, M., Fukuda, T., & Tokuhisa, T. (2008). Role of the Transcriptional Repressor BCL6 in Allergic Response and Inflammation. *World Allergy Organization Journal*, *1*(7), 115–122. https://doi.org/10.1097/wox.0b013e31817dc522

Bacon, A. P., Carter, R. E., Ogle, E. A., & Joyner, M. J. (2013). VO2max Trainability and High Intensity Interval Training in Humans: A Meta-Analysis. *PLoS ONE*, *8*(9). https://doi.org/10.1371/journal.pone.0073182

Barish, G. D., Atkins, A. R., Downes, M., Olson, P., Chong, L. W., Nelson, M., Zou, Y., Hwang, H., Kang, H., Curtiss, L., Evans, R. M., & Lee, C. H. (2008). PPARδ regulates multiple proinflammatory pathways to suppress atherosclerosis. *Proceedings of the National Academy of Sciences of the United States of America*, *105*(11), 4271–4276. https://doi.org/10.1073/pnas.0711875105

Cardenas, M. G., Yu, W., Beguelin, W., Teater, M. R., Geng, H., Goldstein, R. L., Oswald, E., Hatzi, K., Yang, S. N., Cohen, J., Shaknovich, R., Vanommeslaeghe, K., Cheng, H., Liang, D., Cho, H. J., Abbott, J., Tam, W., Du, W., Leonard, J. P., Elemento, O., Cerchietti, L., Cierpicki, T., Xue, F., MacKerell Jr., A. D., & Melnick, A. M. (2016). Rationally designed BCL6 inhibitors target activated B cell diffuse large B cell lymphoma. *Journal of Clinical Investigation*, *126*(9), 3351–3362. https://doi.org/10.1172/JCI85795

Chen, D., Zang, Y. H., Qiu, Y., Zhang, F., Chen, A. D., Wang, J. J., Chen, Q., Li, Y. H., Kang, Y. M., & Zhu, G. Q. (2019). BCL6 attenuates proliferation and oxidative stress of vascular smooth muscle cells in hypertension. *Oxidative Medicine and Cellular Longevity*, *2019*. https://doi.org/10.1155/2019/5018410

Chen, L., & Yang, G. (2014). PPARs integrate the mammalian clock and energy metabolism. *PPAR Research*, *2014*. https://doi.org/10.1155/2014/653017

Ci, W., Polo, J. M., & Melnick, A. (2008). B-cell lymphoma 6 and the molecular pathogenesis of diffuse large B-cell lymphoma. In *Current Opinion in Hematology* (Vol. 15, Issue 4, pp. 381–390). https://doi.org/10.1097/MOH.0b013e328302c7df

Dee, K., Freer, M., Mei, Y., & Weyman, C. M. (2002). Apoptosis coincident with the differentiation of skeletal myoblasts is delayed by caspase 3 inhibition and abrogated by MEK-independent constitutive Ras signaling. *Cell Death and Differentiation*, *9*(2), 209–218. https://doi.org/10.1038/sj/cdd/4400930

Dent, A. L., Shaffer, A. L., Yu, X., Allman, D., & Staudt, L. M. (1997). Control of inflammation, cytokine expression, and germinal center formation by BCL-6. In *Science* (Vol. 276, Issue

5312, pp. 589–592). https://doi.org/10.1126/science.276.5312.589

Ertek, S., & Cicero, A. (2012). Impact of physical activity on inflammation: Effects on cardiovascular disease risk and other inflammatory conditions. *Archives of Medical Science*, *8*(5), 794–804. https://doi.org/10.5114/aoms.2012.31614

Feoktistova, M., Geserick, P., & Leverkus, M. (2016). Crystal violet assay for determining viability of cultured cells. In *Cold Spring Harbor Protocols* (Vol. 2016, Issue 4, pp. 343–346). https://doi.org/10.1101/pdb.prot087379

Füchtbauer, E. -M, & Westphal, H. (1992). MyoD and myogenin are coexpressed in regenerating skeletal muscle of the mouse. *Developmental Dynamics*, *193*(1), 34–39. https://doi.org/10.1002/aja.1001930106

Green, R. (2006). *Closing the loop : p53-BCL6 feedback Protean H pylori : perhaps " pernicious " too ? 107*(4), 15–16.

Hatzi, K., Jiang, Y., Huang, C., Garrett-Bakelman, F., Gearhart, M. D., Giannopoulou, E. G., Zumbo, P., Kirouac, K., Bhaskara, S., Polo, J. M., Kormaksson, M., MacKerell, A. D., Xue, F., Mason, C. E., Hiebert, S. W., Prive, G. G., Cerchietti, L., Bardwell, V. J., Elemento, O., & Melnick, A. (2013). A hybrid mechanism of action for BCL6 in B cells defined by formation of functionally distinct complexes at enhancers and promoters. *Cell Reports*, *4*(3), 578–588. https://doi.org/10.1016/j.celrep.2013.06.016

Hindi, L., McMillan, J., Afroze, D., Hindi, S., & Kumar, A. (2017). Isolation, Culturing, and Differentiation of Primary Myoblasts from Skeletal Muscle of Adult Mice. *Bio-Protocol*, *7*(9). https://doi.org/10.21769/bioprotoc.2248

Hou, L., Zhu, L., Li, H., Jiang, F., Cao, L., Hu, C. Y., & Wang, C. (2019). MiR-501-3p Forms a Feedback Loop with FOS, MDFI, and MyoD to Regulate C2C12 Myogenesis. *Cells*, *8*(6), 573. https://doi.org/10.3390/cells8060573

Khazaei, M. (2012). Chronic low-grade inflammation after exercise: Controversies. *Iranian Journal of Basic Medical Sciences*, *15*(5), 1008–1009. https://doi.org/10.22038/ijbms.2012.4906

Kim, H., Kim, M., Im, S.-K., & Fang, S. (2018). Mouse Cre-LoxP system: general principles to determine tissue-specific roles of target genes. *Laboratory Animal Research*, *34*(4), 147. https://doi.org/10.5625/lar.2018.34.4.147

Kumagai, T., Miki, T., Kikuchi, M., Fukuda, T., Miyasaka, N., Kamiyama, R., & Hirosawa, S. (1999). The proto-oncogene Bcl6 inhibits apoptotic cell death in differentiation-induced mouse myogenic cells. *Oncogene*, *18*(2), 467–475. https://doi.org/10.1038/sj.onc.1202306

Kurata, M., Maesako, Y., Ueda, C., Nishikori, M., Akasaka, T., Uchiyama, T., & Ohno, H. (2002). Characterization of t(3;6)(q27;p21) breakpoints in B-cell non-Hodgkin's lymphoma

and construction of the histone H4/BCL6 fusion gene, leading to altered expression of Bcl-6. *Cancer Research*, *62*(21), 6224–6230.

LaPensee, C. R., Lin, G., Dent, A. L., & Schwartz, J. (2014). Deficiency of the transcriptional repressor B cell lymphoma 6 (Bcl6) is accompanied by dysregulated lipid metabolism. *PLoS ONE*, *9*(6). https://doi.org/10.1371/journal.pone.0097090

Liberti, M. V, & Locasale, J. W. (2016). The Warburg Effect: How Does it Benefit Cancer Cells? (vol 41, pg 211, 2016). *Trends in Biochemical Sciences*, *41*(3, SI), 287. https://doi.org/10.1016/j.tibs.2016.01.004

Lodish, H., Berk, A., Zipursky, S. L., & Al., E. (2000). Electron Transport and Oxidative Phosphorylation - Molecular Cell Biology - NCBI Bookshelf. In *Molecular Cell Biology* (p. Section 16.2). https://www.ncbi.nlm.nih.gov/books/NBK21528/

M. Christopher, A. M. L. S. (2016). 乳鼠心肌提取 HHS Public Access. *Physiology & Behavior*, *176*(1), 100–106. https://doi.org/10.1016/j.gde.2016.03.011

Malumbres, M. (2014). *Cyclin-dependent kinases*. 1–10.

Muñoz-Alonso, M. J., Acosta, J. C., Richard, C., Delgado, M. D., Sedivy, J., & León, J. (2005). p21Cip1 and p27Kip1 induce distinct cell cycle effects and differentiation programs in myeloid leukemia cells. *Journal of Biological Chemistry*, *280*(18), 18120–18129. https://doi.org/10.1074/jbc.M500758200

Murphy, M., Robertson, W., Javed, S., Leader, M., Kay, E., Murphy, G. M., Mabruk, M. J. E. M. F., Lenane, P., Liew, A., McCann, P., Buckley, A., Flatharta, C. O., Hevey, D., & Billet, P. (2002). Comparison of the expression of p53, p21, Bax and the induction of apoptosis between patients with basal cell carcinoma and normal controls in response to ultraviolet irradiation. *Journal of Clinical Pathology*, *55*(11), 829–833. https://doi.org/10.1136/jcp.55.11.829

Nance, J. P., Bélanger, S., Johnston, R. J., Hu, J. K., Takemori, T., & Crotty, S. (2015). Bcl6 middle domain repressor function is required for T follicular helper cell differentiation and utilizes the corepressor MTA3. *Proceedings of the National Academy of Sciences of the United States of America*, *112*(43), 13324–13329. https://doi.org/10.1073/pnas.1507312112

Nevins, J. R. (2001). The Rb/E2F pathway and cancer. *Human Molecular Genetics*, *10*(7), 699–703. https://doi.org/10.1093/hmg/10.7.699

Oeckinghaus, A., & Ghosh, S. (2009). The NF-kappaB family of transcription factors and its regulation. *Cold Spring Harbor Perspectives in Biology*, *1*(4), 1–14. https://doi.org/10.1101/cshperspect.a000034

Oestreich, K. J., Read, K. A., Gilbertson, S. E., Hough, K. P., Mcdonald, W., Krishnamoorthy, V., Weinmann, A. S., & Tech, V. (2015). *Bcl-6 directly represses the gene program of the*

glycolysis pathway. *15*(10), 957–964. https://doi.org/10.1038/ni.2985.Bcl-6

Ohno, H. (2006). Pathogenetic and clinical implications of non-immunoglobulin ; BCL6 translocations in B-cell non-Hodgkin's lymphoma. *Journal of Clinical and Experimental Hematopathology : JCEH*, *46*(2), 43–53. https://doi.org/10.3960/jslrt.46.43

Pasqualucci, L., Migliazza, A., Basso, K., Houldsworth, J., Chaganti, R. S. K., & Dalla-Favera, R. (2003). Mutations of the BCL6 proto-oncogene disrupt its negative autoregulation in diffuse large B-cell lymphoma. *Blood*, *101*(8), 2914–2923. https://doi.org/10.1182/blood-2002-11-3387

Pomerening, J. R. (2008). Positive Feedback Loops in Cell Cycle Progression. *Bone*, *23*(1), 1–7. https://doi.org/10.1038/jid.2014.371

Puvion-Dutilleul, F., Souquere-Besse, S., & Albagli-Curiel, O. (2003). The relationship between BCL6 bodies and nuclear sites of normal and halogenated DNA and RNA synthesis. *Microscopy Research and Technique*, *61*(4), 389–407. https://doi.org/10.1002/jemt.10363

Roberts, L. D., Ashmore, T., McNally, B. D., Murfitt, S. A., Fernandez, B. O., Feelisch, M., Lindsay, R., Siervo, M., Williams, E. A., Murray, A. J., & Griffin, J. L. (2017). Inorganic nitrate mimics exercise-stimulated muscular fiber-Type switching and myokine and g-Aminobutyric acid release. *Diabetes*, *66*(3), 674–688. https://doi.org/10.2337/db16-0843

Ruas, J. S., Siqueira-Santos, E. S., Amigo, I., Rodrigues-Silva, E., Kowaltowski, A. J., & Castilho, R. F. (2016). Underestimation of the maximal capacity of the mitochondrial electron transport system in oligomycin-treated cells. *PLoS ONE*, *11*(3), 1–20. https://doi.org/10.1371/journal.pone.0150967

Salmond, R. J. (2018). mTOR regulation of glycolytic metabolism in T cells. *Frontiers in Cell and Developmental Biology*, *6*(SEP), 1–9. https://doi.org/10.3389/fcell.2018.00122

Samavati, L., Lee, I., Mathes, I., Lottspeich, F., & Hüttemann, M. (2008). Tumor necrosis factor α inhibits oxidative phosphorylation through tyrosine phosphorylation at subunit I of cytochrome c oxidase. *Journal of Biological Chemistry*, *283*(30), 21134–21144. https://doi.org/10.1074/jbc.M801954200

Senagolage, M. D., Sommars, M. A., Ramachandran, K., Futtner, C. R., Omura, Y., Allred, A. L., Wang, J., Yang, C., Procissi, D., Evans, R. M., Han, X., Bederman, I. R., & Barish, G. D. (2018). Loss of Transcriptional Repression by BCL6 Confers Insulin Sensitivity in the Setting of Obesity. *Cell Reports*, *25*(12), 3283-3298.e6. https://doi.org/10.1016/j.celrep.2018.11.074

Sharma, A., Agarwal, M., Kumar, A., Kumar, P., Saini, M., Kardon, G., & Mathew, S. J. (2018). *Myosin Heavy Chain-embryonic is a crucial regulator of skeletal muscle development and differentiation*. 1–50.

Shi, Y., Kuai, Y., Lei, L., Weng, Y., Berberich-Siebelt, F., Zhang, X., Wang, J., Zhou, Y., Jiang, X., Ren, G., Pan, H., Mao, Z., & Zhou, R. (2016). The feedback loop of LITAF and BCL6 is involved in regulating apoptosis in B cell non-Hodgkin's-lymphoma. *Oncotarget*, *7*(47), 77444–77456. https://doi.org/10.18632/oncotarget.12680

Smith, R. W., Coleman, J. D., Thompson, J. T., & Vanden Heuvel, J. P. (2016). Therapeutic potential of GW501516 and the role of Peroxisome proliferator-activated receptor β/δ and B-cell lymphoma 6 in inflammatory signaling in human pancreatic cancer cells. *Biochemistry and Biophysics Reports*, *8*(October), 395–402. https://doi.org/10.1016/j.bbrep.2016.10.014

Sommars, M. A., Ramachandran, K., Senagolage, M. D., Futtner, C. R., Germain, D. M., Allred, A. L., Omura, Y., Bederman, I. R., & Barish, G. D. (2019). Dynamic repression by BCL6 controls the genome-wide liver response to fasting and steatosis. *ELife*, *8*, 1–25. https://doi.org/10.7554/eLife.43922

Tanaka, K., Sato, K., Yoshida, T., Fukuda, T., Hanamura, K., Kojima, N., Shirao, T., Yanagawa, T., & Watanabe, H. (2011). *Evidence for cell density affecting C2C12 myogenesis_ possible regulation of myogenesis by cell–cell communication - Tanaka - 2011 - Muscle & Nerve - Wiley Online Library* (pp. 968–977). Muscle & Nerve. https://onlinelibrary.wiley.com/doi/abs/10.1002/mus.22224

Thomas, M. A., Krajcsi, P., Lichtenstein, D. L., Tollefson, A. E., & Wold, W. S. M. (2006). 121. Adenovirus Titers Determined by Quantitative Real-Time PCR Correlate with Infectious Titers. *Molecular Therapy*, *13*(May), S49–S50. https://doi.org/10.1016/j.ymthe.2006.08.142

Tower, J. (2008). Stress and Stem Cells. *Bone*, *23*(1), 1–7. https://doi.org/10.1038/jid.2014.371

Vilventhraraja, E., Klymenko, T., Edelmann, J., Gribben, J., & Ivanov, A. (2016). Reduction of Mitochondrial Membrane Potential Leads to Enhancement of Type-II CD20-Antibody Cytotoxicity in Diffuse Large B-Cell Lymphoma. *Blood*, *128*(22), 1763. https://doi.org/10.1182/blood.V128.22.1763.1763

Wagner, S. D., Ahearne, M., & Ferrigno, P. K. (2011). The role of BCL6 in lymphomas and routes to therapy. *British Journal of Haematology*, *152*(1), 3–12. https://doi.org/10.1111/j.1365-2141.2010.08420.x

Wang, L., Duan, Q., Wang, T., Ahmed, M., Zhang, N., Li, Y., Li, L., & Yao, X. (2015). Mitochondrial respiratory chain inhibitors involved in ROS production induced by acute high concentrations of iodide and the effects of sod as a protective factor. *Oxidative Medicine and Cellular Longevity*, *2015*. https://doi.org/10.1155/2015/217670

Weimer, K., & DiMario, J. X. (2017). Muscle Fiber Type Specific Activation of the Slow Myosin Heavy Chain 2 Promoter by a Non-canonical E-box. *Physiology & Behavior*, *176*(1), 139–148. https://doi.org/10.1016/j.physbeh.2017.03.040

Wright, E., Scism-Bacon, J. L., & Glass, L. C. (2006). Oxidative stress in type 2 diabetes: The role of fasting and postprandial glycaemia. *International Journal of Clinical Practice*, *60*(3), 308–314. https://doi.org/10.1111/j.1368-5031.2006.00825.x

Wu, C. C., Baiga, T. J., Downes, M., La Clair, J. J., Atkins, A. R., Richard, S. B., Fan, W., Stockley-Noel, T. A., Bowman, M. E., Noel, J. P., & Evans, R. M. (2017). Structural basis for specific ligation of the peroxisome proliferator-activated receptor δ. *Proceedings of the National Academy of Sciences of the United States of America*, *114*(13), E2563–E2570. https://doi.org/10.1073/pnas.1621513114

Yu, B. C., Chang, C. K., Ou, H. Y., Cheng, K. C., & Cheng, J. T. (2008). Decrease of peroxisome proliferator-activated receptor delta expression in cardiomyopathy of streptozotocin-induced diabetic rats. *Cardiovascular Research*, *80*(1), 78–87. https://doi.org/10.1093/cvr/cvn172

Zhang, H., Qi, X., Wu, J., Huang, X., Zhang, A., Chen, S., Ding, X. C., Le, S., Zou, Y., Xu, H., Ye, P., & Xia, J. (2019). BCL6 inhibitor FX1 attenuates inflammatory responses in murine sepsis through strengthening BCL6 binding affinity to downstream target gene promoters. *International Immunopharmacology*, *75*(July), 105789. https://doi.org/10.1016/j.intimp.2019.105789